The Slag-Metal Interface and Associated Phenomena

by

A. W. Cramb*, Y. Chung*, J. Harman*, A. Sharan** and I. Jimbo***

*Department Of Materials Science and Engineering Carnegie Mellon University, Pittsburgh, Pa 15213, **Homer Research Laboratories, Bethlehem Steel Corp., Pa 18016, ***Department of Materials Science and Engineering, Tokai University, Kanagawa, Japan

Abstract

The slag-metal interface is the site of many of the most important metallurgical phenomena that occur during the processing of liquid steels. Emulsification of liquid slag, separation of liquid slag from liquid iron alloys and the refining of liquid iron alloys are examples of processes that are dependent upon a detailed knowledge of slag-metal interfacial phenomena, if they are to be controlled. In particular, the interfacial tension between a liquid slag and a liquid iron alloy must be known in order to control the above processes. In the measurement of interfacial energies most studies are carried out under equilibrium conditions between the liquid slag and the metal; however, most industrial processes are carried out under non-equilibrium conditions and measurements of steady state or transient interfacial tensions during reaction between a liquid metal and a slag indicate that non-equilibrium values of interfacial tension can vary significantly when compared to equilibrium values. In this paper, our current understanding of the state of knowledge concerning the interfacial tension of liquid slag- liquid iron alloys will be presented and recent results from measurements of samples used in industrial operations will be presented.

Introduction

During the operation of steel refining vessels, of the tundish and of the continuous casting mold, the onset of slag emulsification during processing can often be related to product defects in continuously cast billets, slabs and blooms[1-25]. It is often the goal of steel processors to eliminate the occurrence of inclusions whose diameters are larger than 20 microns. In Table 1, from the review of Marukawa[26] , it can be seen that there are a number of high purity and cleanliness requirements by grade and application and these steels are marked by the requirement that permissible inclusion diameters must be lower than 20 microns. Emulsification of the covering slags used in steel processing is a common source of inclusions that are larger than 20 microns in diameter.

Emulsification of slag in steel processing occurs due to shear at the slag-metal interface caused by excessive liquid steel flow. The onset of emulsification is also a function of the slag properties: viscosity, density and interfacial tension[5]. Therefore, the onset of emulsification tends to be related to the sub-meniscus fluid velocity, the shear

length (often related to slag depth) and the slag physical properties. Due to these controlling factors the onset of emulsification is very practice specific and varies from plant to plant. There are however five processing conditions where emulsification can be expected:

1. vessel filling where there are very high pouring energies in the steel stream and the stream is poured through the slag
2. vessel drainage where vortexing can occur
3. Excessive turbulence at the slag metal interface due to wave motion or stream impingement on a container wall that causes upward flow of the steel stream towards the slag-metal interface.
4. Gas injection at rates that exceed a critical value
5. Interfacial level fluctuations that exceed a critical level

These conditions can lead to the production of continuous cast steels that contain sporadic spherical inclusions of a diameter that varies between 20 and 500 microns, depending upon the processing conditions. Thus to produce clean steels via continuous casting slag emulsification in the ladle, tundish and mold must be eliminated.

There are two methods by which slag emulsification during processing can be controlled: by controlling fluid flow or by slag design. This paper will focus upon the role of slag-metal interfacial tension on emulsification

Background

Emulsification of slags in continuous casting is well recognized as the route cause of certain surface defects on continuous cast slabs and certain line defects, often called slivers or laminations, that are found on the sheet material rolled from continuous cast slabs. The fluid flow conditions leading to emulsification have been well documented[4]

Table 1: Requirements for High Purity and Ultra Clean Steels [26]

Product	Purity	Clean-liness	Notes
Auto-motive Sheet	C < 30 ppm N < 30 ppm	T[O] < 20 ppm d < 100 μm	Ultra deep drawing appli-cations
Drawn and Ironed Cans		T[O] < 20 ppm d < 20 μm	Two piece beverage and battery cans
Lead frame for LSI	N < 50 ppm	d < 5 μm	Crack prevent-ion in punch forming
Shadow Mask for CRT		d < 5 μm	Prevention of Photo Etching
Tire Cord		d < 20 μm of non-plastic inclusions	Prevent-ion of rupture in wire drawing
Ball Bearings	[Ti] < 15 ppm	T [O] < 10 ppm d < 15 μm	Increased fatigue life
Line pipe	S < 10 ppm	d < 100 μm oxide shape	Sour gas service

and include vortexing, downward shear flow at the slag metal interface and pouring through a slag layer. A schematic example from high speed continuous slab casting is shown in

Figure 1 where emulsification occurs at higher SEN submersion depths and higher cast speeds at the edges of the slab due to excessive flow up the narrow face of the mold. The effect of fluid physical properties on emulsification has been extensively studied by Feldbauer[5] and Harman[6] who have both shown that the critical shear conditions for emulsification are controlled by slag viscosity, interfacial tension and slag volume. The mechanism of emulsification is that the slag is drawn with the steel flow until a long tendril forms. This tendril extends as the sub-meniscus fluid velocity increases and tends to curve upwards. Eventually, at a significant distance from the initial interface, a capillary instability occurs in the extended slag tendril and a droplet is released into the steel stream. If the sub-meniscus velocity is increased past this point, droplets are produced continuously and the droplet size distribution increases.

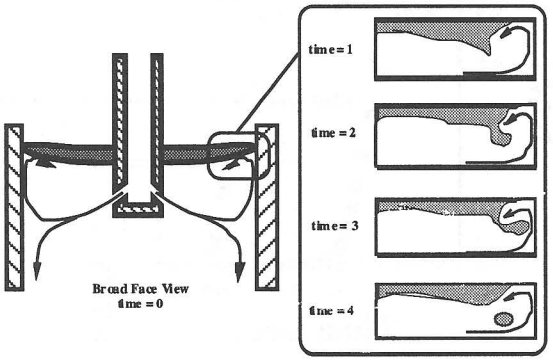

Figure 1: Schematic of Slag Emulsification at High Casting Speeds in a Continuous Slab Caster

For example, Harman has shown that both the onset of emulsification and the initial droplet size is strongly related to the interfacial tension between the fluids (Figures 2 and 3) in studies of the emulsification of silicon oil in water, and, by dimensional analysis, has calculated that the interfacial energy is a key parameter in the emulsification of mold slags (Figure 4)[6].

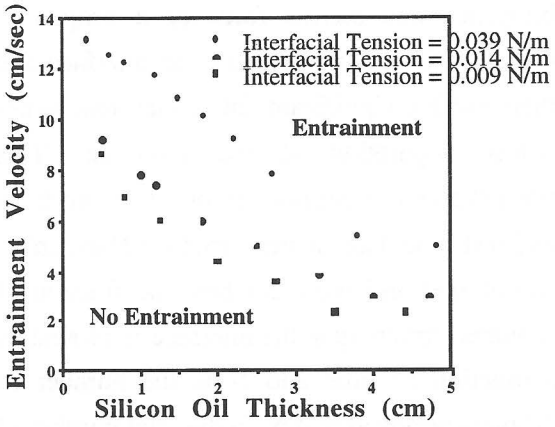

Figure 2: Emulsification Velocity Profiles as a Function of Silicon Oil Thickness and Interfacial Tension at the Silicon Oil - Water Interface[5]

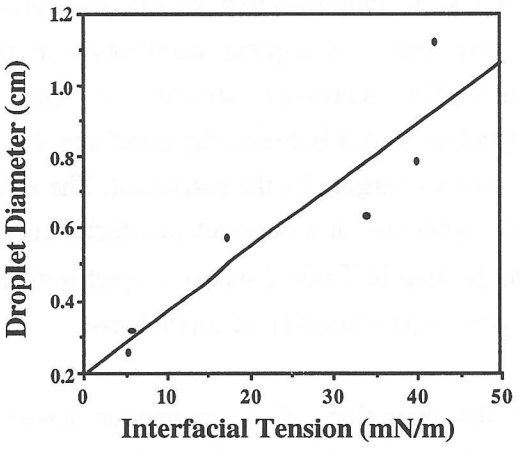

Figure 3: Initial Silicon Oil Droplet Diameter as a Function of Interfacial Tension[5]

In addition to emulsification, separation of emulsified liquid droplets at a liquid-liquid interface can be related to phenomena associated with the interfacial energy between liquids. For example, when the interfacial tension of a liquid-liquid interface is greater than the buoyancy force or the combined buoyancy and inertial force of a droplet, a droplet will initially spread at an interface and then exhibit significant interfacial rest times before separation at the interface. This phenomena is common in oil-water systems and rest time data, as measured by Harman[26], can be seen in Figure 5 where the fraction of droplets remaining at the interface is plotted as a function of time and N is the number of droplets removed and N_o is the total number of droplets (450) in the study. The statistical nature of droplet coalescence at an interface can be seen in Figure 5 for a silicon oil droplet of diameter 0.35 cm coming into contact with a silicon oil/ water interface. The effect of varying interfacial energy can also be seen in Figure 5 where the addition of an alcohol based surfactant leads to a reduction in surface energy and a subsequent stabilization in rest time. The increased stability is due to repulsion forces between the interfaces due to interface charging by the surfactant. The effect of droplet size at a constant interfacial energy can be seen in Table 2 where droplet rest time increases as a function of droplet size.

In the operation of a continuous caster a knowledge of the actual interfacial tension under operational conditions will be a key to understanding the defect free production of slabs from a continuous caster.

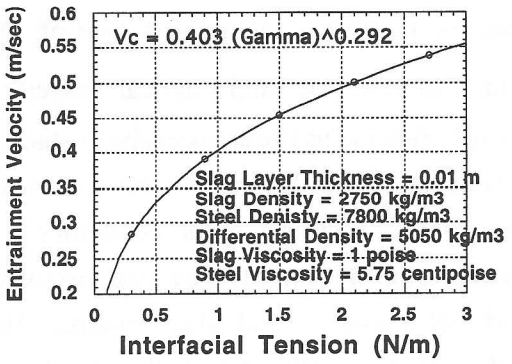

Figure 4: Calculated Variation of Sub-Meniscus Velocity in the Mold of a Continuous Caster as a Function of Interfacial Tension[5]

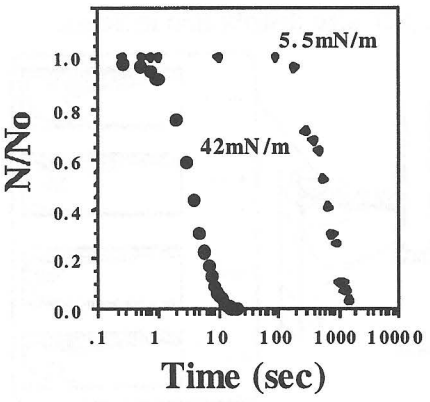

Figure 5: Fraction of Droplets Remaining at a Silicon Oil /Water Interface as a Function of Time and Interfacial Tension

Table 2: Statistical Variance of Silicon Oil Droplet Rest Times

Mean Droplet Diameter (cm)	Average Rest Time (sec)	Standard Deviation of Average Rest Time
0.35	3.83	3.0
0.59	6.42	3.4
1.14	2.94	1.5
1.52	6.01	3.5
All Drops	4.37	3.2

Equilibrium Surface and Interfacial Energies

It is well known that oxygen and sulfur in liquid iron are surface active and that the surface tension of liquid iron at constant temperature decreases with increasing sulfur and oxygen contents. In Figure 6, the data of three investigators[28-32], whose results are practically identical, are plotted for the iron-sulfur system at 1550 C. Figure 7 shows similar results for the iron-oxygen system at 1550 C[33-36] and in these figures both sulfur and oxygen are seen to cause drastic reductions in the surface tension of liquid iron.

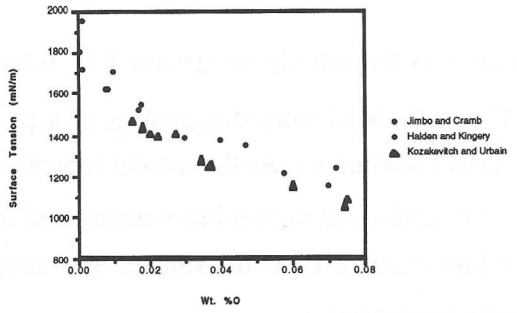

Figure 6: Effect of Oxygen on the Surface Tension of Iron

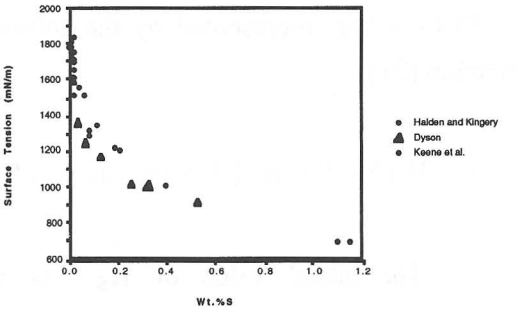

Figure 7: Effect of Sulfur on the Surface Tension of Iron

The first empirical relationship to account for the effect of surface active elements in liquids was developed by Szyszkowski in 1908[37] ;however, use of this relationship did not become widespread until Belton[38] derived a similar relation by combining the Gibbs adsorption isotherm with that of Langmuir:

$$\gamma = \gamma^0 - R\,T\,\Gamma^0 \ln\left[1 + K_i\,.a_i\right] \quad \ldots [1]$$

where γ^0 is the surface tension of pure iron, Γ^0 is the surface excess at saturation, K_i is the adsorption coefficient of species **i**

and a_i is the activity of species i in solution. Γ^0 is calculated from the gradient of a plot of surface tension verses the natural logarithm of solute activity at high solute contents and if γ^0 is known, then K_i is determined by fitting the data to equation 1.

Taking into account the more recent determination of the surface tension of pure iron[36] and other studies, the data for the effect of sulfur on the surface tension of pure iron at 1550 C is best represented by the following relation [21]:

$$\gamma = 1913 - 195 \ln [1 + 365\ a_S] \quad \ldots [2]$$

The actual value of K_S is very sensitive to the value taken for pure liquid iron. Belton's previous interpretation of the data used Kozakevich's value[27] of 1788 mN/m for the value for pure liquid iron and derived a value of 185 for the adsorption coefficient of sulfur on liquid iron. Re-evaluation of the data allows the starting point for the effect of sulfur to be coincident with the starting point for the effect of oxygen. The effect of oxygen on the surface tension of liquid iron at 1550 C can be expressed as:

$$\gamma = 1913 - 279 \ln [1 + 140\ a_O] \quad \ldots [3]$$

Other elements such as chromium[39] and nickel[40,41], that are common in stainless steels, have only small effects on the surface tension of liquid iron at low oxygen contents (Figures 8 and 9); however, at higher oxygen contents Fe-Ni alloys exhibit a quite anomalous non-ideal behavior (Figure 9) where decreased surface tension with increasing oxygen content is apparent at low nickel contents but not at higher nickel contents.

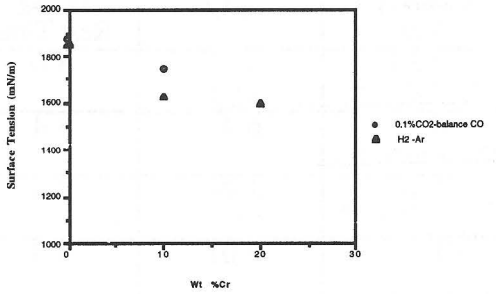

Figure 8: Effect of Chromium on the Surface Tension of Iron[39]

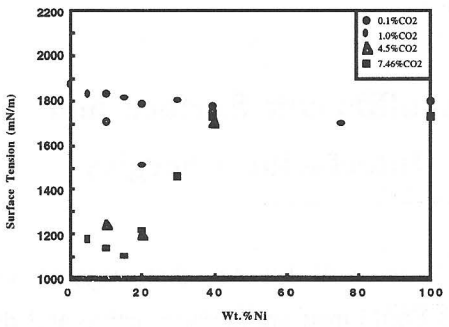

Figure 9: Effect of Increasing CO_2/CO Ratio on the Surface Tension of Fe-Ni Alloys [40]

The effect of nitrogen on surface tension is slight and an example can be seen in Figure 10 for increasing nitrogen contents in an Fe-20% Cr alloy at 1550°C[24] . The effect of nitrogen on pure iron alloys is similar to that seen in Figure 10. In Figure 11 the strong effect of large additions of silicon to the surface and interfacial tension of liquid iron was shown by Dumay[41].

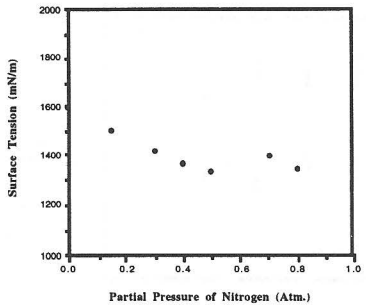

Figure 10: Effect of Nitrogen on the Surface Tension of an Fe-20% Cr Alloy [39]

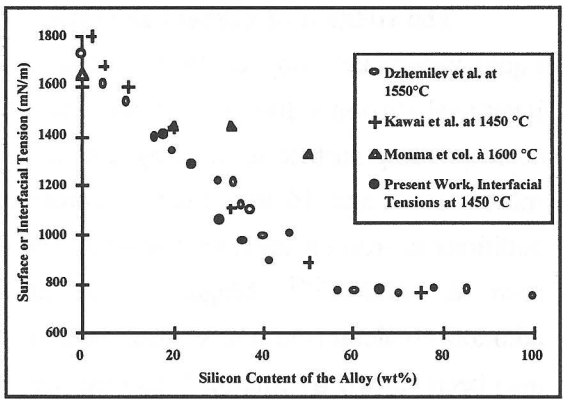

Figure 11: Surface and Interfacial Tensions in Fe-Si Alloys[40]

Equilibrium interfacial energies in steel-slag systems, where a slag is added to predominantly iron alloys, are generally 200 - 300 mN/m less than the corresponding surface tensions of the iron alloys due to an associative interaction between the slag and the metal surface that leads to the reduction in interfacial energy. The interfacial energy reduction leads to the wetting of slag droplets on liquid steels.

Values for equilibrium interfacial tensions between liquid iron and liquid iron-nickel alloys and lime-alumina-silica slags are given in Figure 12[35,40]. Under these conditions equilibrium between the slag and steel leads to not only varying slag composition but also varying alloy oxygen content. Thus higher silica contents in the slag are equivalent to higher oxygen contents in the metal and the effect of silica additions to the slag are magnified in equilibrium studies [36] . In general interfacial tension increases with increasing slag alumina content.

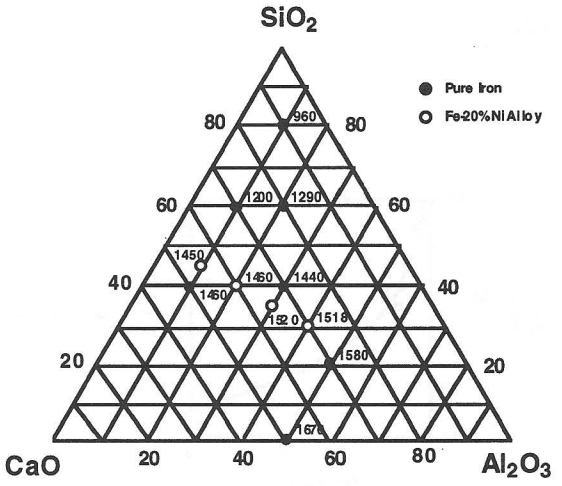

Figure 12: Interfacial Tensions between Liquid Iron and Liquid Fe-20% Ni Alloys and Lime-Alumina Silica Slags at 1550°C [40]

Major effects in interfacial tension are caused by variations in equilibrium oxygen content or sulfur content in a manner similar to the effects measured on the surface tension of pure iron. In equilibrium experiments dissolved oxygen and FeO in the slag are related; therefore, the interfacial tension can be plotted either as a function of oxygen activity or FeO content of the slag.

For example, from the data of Gaye et al.[44] , the effect of slag FeO content on

interfacial tension is plotted in Figure 13 for lime-silica-alumina-iron oxide slags in equilibrium with pure iron, and a large reduction in interfacial tension can be seen as the iron oxide content increases[44]. The effect of sulfur in interfacial tension is similar to oxygen (Figure 14), again taken from the data of Gaye et al.[44]. At low sulfur and oxygen contents (< 10 ppm) the effect of the addition of a calcium aluminate slag addition to iron-nickel alloys at 1550 C can be seen in Figure 15.

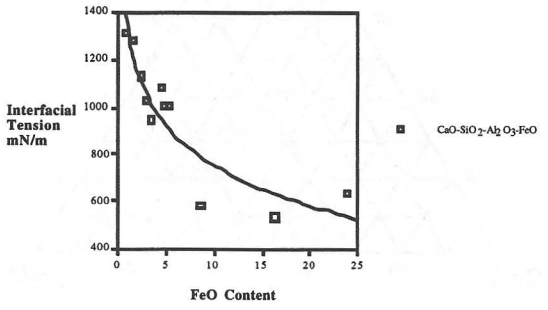

Figure 13: Effect of FeO Content on Interfacial Tension [44]

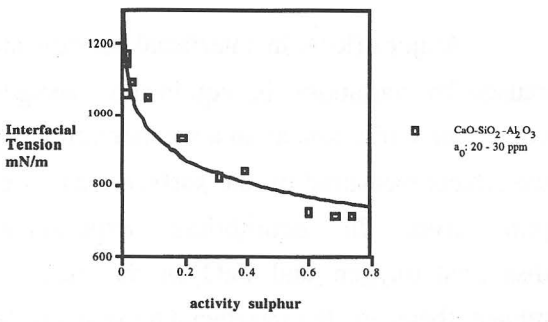

Figure 14: Effect of Steel Sulfur Content on Interfacial Tension [44]

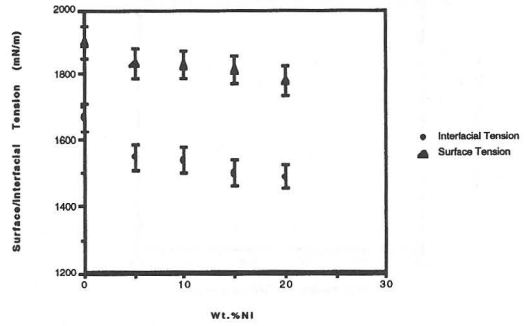

Figure 15: Effect of Addition of Calcium Aluminate to Iron-Nickel Alloys [39]

The addition of calcium aluminate to a liquid iron-nickel alloy at 1600°C causes an interfacial tension value that is lower than the corresponding surface tension by 200 to 300 mN/m. In Figure 16 the effect of chromium additions to iron on interfacial tension can be seen at 1600 C[39]. Magnesia and titania addition to calcium aluminate based slags have also been shown by Sharan[41] to significantly decrease interfacial energies and an example is given in Figure 17.

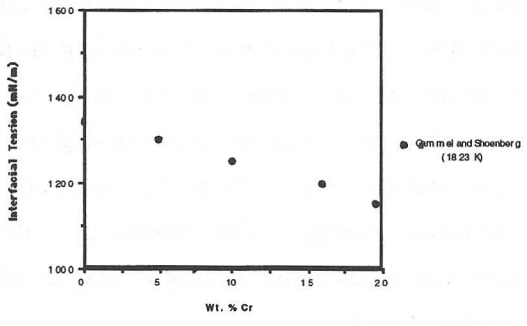

Figure 16: Effect of Chromium on Interfacial Tension[43]

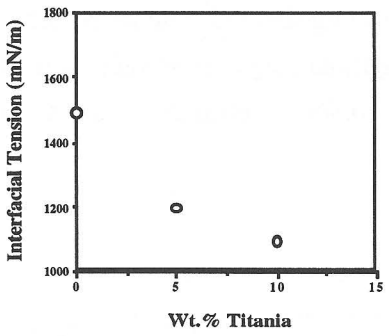

Figure 17: Effect of Titania on Interfacial Tension[41]

Thus, equilibrium interfacial tensions can vary from 1670 mN/m to 600 mN/m depending upon the solute content of the metal and the slag chemistry

Non-Equilibrium Effects on Interfacial Energies

One of the most problematic issues in measuring the surface or interfacial tension of any system is that it is essential to ensure that mass transfer between the phases is eliminated. As has been shown by numerous investigators[44, 45], reaction between the two phases can lead to either lowered or increased values of surface or interfacial tension, where both effects can be measured as a function of time during an experiment. This phenomena can be seen in Figure 18 where the droplet shape is not constant with time as the aluminum in the alloy reacts with the silica in the slag. One of the major problems in attempting to develop practical values for interfacial tension is that in reality most slag-metal systems are reacting and that the actual interfacial tension is varying with time until some steady state value can be measured. The concept of applying an equilibrium measurement to an industrial system is thus potentially flawed, if the reaction between the phases is significant.

It is thus necessary to measure interfacial tensions in real systems over a significant time frame and for this reason a new experimental technique was developed to allow in excess of 2 hours of experimental time and the determination of a steady state value for a slightly reacting system[46]. All measurements of slag metal interfacial tension for chemistries similar to industrial systems tend to give a steady state value as equilibrium is rarely reached between the steel and the slag.

In an attempt to measure a reasonable value of interfacial tension for the conditions found in the mold of a continuous caster, the interfacial tensions for flux chemistries in the $CaO\text{-}SiO_2\text{-}Na_2O\text{-}CaF_2$ family in contact with a 304 stainless steel were determined by Chung[47]. The interfacial tension value between a 304 stainless steel (Table 3) and the mother slag of composition $CaO\text{-}45\%SiO_2\text{-}20\%CaF_2$ was 940 mN/m and was substantially lower than that for the same 304 steel grade in contact with $CaO\text{-}SiO_2$ (1:1) (ca. 1450 mN/m) and calcium aluminate (ca. 1550 mN/m). Values are based upon average steady state measurements over at least 1 hour after all phases are liquid.

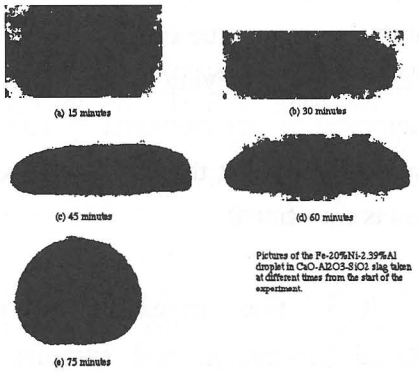

Figure 18: Effect of Mass Transfer Upon Droplet Shape and Apparent Interfacial Energy [41].

Figure 19 shows the effect of Na_2O or Al_2O_3 additions to the mother slag (Table 4) on the interfacial tension between the slags and a SUS 304 steel. Increases in the Al_2O_3 content of the slags lead to a higher steady state value of interfacial tension between the slag and the stainless steel. A substantial decrease in interfacial tension between the slag and the stainless steel can be observed on the addition of Na_2O to the mother slag. These results are steady state measurements as the 304 stainless steel is not in equilibrium with the slag. This result indicates that the addition of calcium fluoride can significant depress interfacial energy; however, as alumina is added to the mother slag (Figure 19) the effect of calcium fluoride on interfacial tension is reduced and the interfacial tension increases towards that measured for lime-silica-alumina alloys in equilibrium with pure iron. The addition of sodium oxide and sodium oxide can lead to extremely low values of interfacial tension indicating that the interfacial tensions in operating mold slags could vary from 600 to 1600 mN/m depending upon slag chemistry.

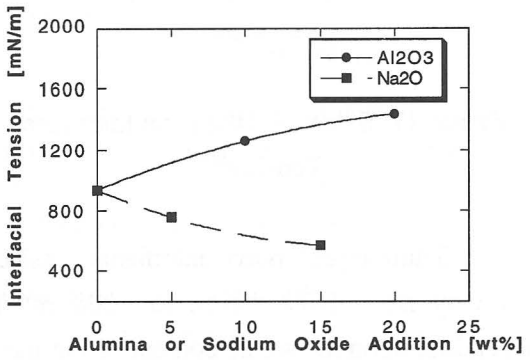

Figure 19: Effect of Sodium Oxide or Alumina Additions to a Slag Containing 20% CaF_2 [46]

A number of measurements of interfacial tensions between industrial carbon steels and actual mold slags were also undertaken by Chung[47]. Figure 20 shows the interfacial tension between industrial carbon and ultra low carbon steels (Table 7) and actual mold slags supplied by company 1 at the 1550 °C as a function of time. The average values of these samples ranged from 980[mN/m] to 1350[mN/m]. These differences can be understood by the analysis of slag compositions in Table 5 where those mold slag compositions with highest total amounts of F and Na_2O resulted in lower interfacial tensions.

Table 3. The Composition of 304 Stainless Steel

C	Mn	P	S	Si	Cr	Ni	Mo
.057	1.83	.027	.005	0.45	18.5	8.10	0.31
Co	Cb	Al	Ti	Sn	Pb	O	N
0.11	.006	.001	.001	.014	.001	.005	.055

Table 4. The Composition of Slags (wt %)

	SiO_2	CaO	CaF_2	Na_2O	Al_2O_3
A	45.0	35.0	20.0		
B	40.0	31.5	18.0		10.0
C	36.0	28.0	16.0		20.0
D	42.5	33.5	19.0	5.0	
E	38.3	29.7	17.0	15.0	

Table 5: Mold Slag Compositions Supplied by Company 1

Species / Sample	A	B	C	D
CaO	27.7	29.0	32	35.9
SiO_2	33.1	34.6	33	39.9
F	8.3	9.3	6.8	7.3
Na_2O	12.3	11.7	10.5	2.3
MgO	1.2	1.3	0.7	5.6
C	6.4	4.1	6.6	3.8
CaO/SiO_2	0.84	0.84	0.90	0.97

Table 6. Mold Slag Compositions Supplied by Company 2. (u means sampled from mold)

	Slag 1	Slag 1u	Slag 2	Slag 2u	Slag 3	Slag 3u	Slag 4	Slag 4u
CaO	37.6	40.8	30.5	31.7	33.6	33.7	34.7	36.9
SiO_2	37.6	32.6	36.3	35.9	38.5	35.2	37.5	35.6
F	10.6	12.2	5.4	4.7	6.6	5.6	8.7	8.9
Na_2O	4.6	6.0	4.6	5.02	4.9	5.05	1.9	2.28
MgO	0.8	1.47	6.0	6.32	7.8	7.24	5.2	9.5
C	3.4	-	2.7	-	1.9	-	0.9	-
Al_2O_3	2.7	7.7	5.2	10.9	6.0	11.2	6.8	8.9
Fe_2O_3	3.06	0.9	1.0	0.65	0.6	0.57	1.5	0.85
MnO	4.72	3.81	3.5	2.3	0.6	0.87	0.04	0.93
TiO_2	0.07	1.93	-	2.02	-	0.47	0.2	0.47
Li_2O	-	-	0.7	-	-	-	-	-
K_2O	0.14	0.11	0.5	0.71	0.7	0.92	0.4	0.54
ZrO_2	-	0.73	-	0.35	-	0.48	-	0.23
Basicity	1.09		0.84		0.87		0.93	

Table 7. Composition of Ultra Low Carbon Steel Sample

	Mn	P	S	Si	Al	Ti	C
wt%	0.16	.008	.012	.009	.004	.075	.003

Figure 20 shows the variation of interfacial tensions between one steel sample (Table 7) and the four mold slags supplied by company 2 at 1550 °C as a function of time. These interfacial tensions ranged from 1143 mN/m to 1312 mN/m. Although a small fluctuation can be seen with time, the average values for Slag 1 and Slag 2 have lower interfacial tension values than those of Slag 3 and Slag 4. As can be seen in Table 6, the effect of industrial slag composition on interfacial tension is more difficult to analyze in this case because the slag formulations are composed of more 10 components. If the total amounts of Na_20, F , Fe_2O_3 and MnO are considered, it appears that interfacial tension is strongly influenced by the reducible oxide content of the mold flux.

Company 2 supplied both the flux before use and the flux sampled from the mold during use (Table 6). Interfacial tensions between the steel sample of Table 7 and the used mold slags (sampled from the mold) were measured and results are shown in Figure 21 where results are compared to results using prefused but unused slags. All sampled mold slags (except slag 4) have a larger interfacial tension value than original mold slags. In the case of slag 4, interfacial tension decreased after use. The increases in interfacial tension of slag 1, slag 2 and slag 3 can be explained by the increases of alumina contents during processing. The alumina content of those slags increased about 5 wt% during casting while that of slag 4 increased just 2 wt %. In the case of slag 4, the increase of MgO content, due perhaps to the passage of ladle or tundish slag into the mold, probably caused the decreased interfacial tension.

The actual value of interfacial tension during steel processing can be quite variable and depends upon the actual slag and steel chemistries found during operation. Mass transfer can cause increasing or decreasing interfacial energies depending upon the details of the interfacial conditions. Fluxes containing highly reducible oxides tend to produce low interfacial tensions in practice and it appears that reductions in calcium fluoride and sodium oxide and increases in the alumina content of fluxes are efficient in increasing interfacial tension in practical fluxes.

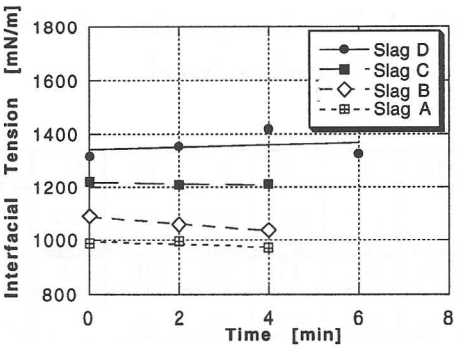

Figure 20: Interfacial Tension Values Between Carbon Steels and Mold Slags, Company 1

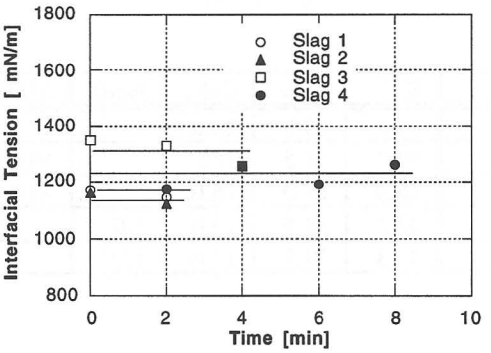

Figure 21: Interfacial Energies Between Carbon Steels and Mold Flux, Company 2

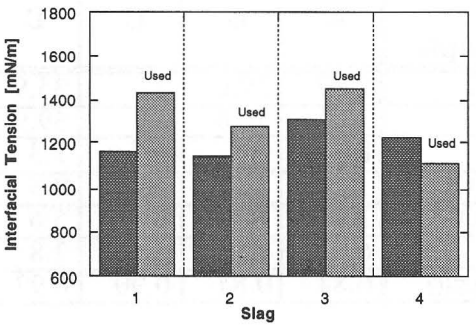

Figure 22: Comparison of Interfacial Tension Values Between Unused and Used Flux.

Conclusion

Interfacial energies in actual industrial systems vary greatly with the exact slag chemistry that is found in the mold of the continuous caster and also as a function of time. Steady state interfacial values were measured to range between 600 and 1400 mN/m for fluxes in contact with industrial steels. Reduction of the calcium fluoride and sodium oxide content and increase of the alumina content of fluxes tends to increase interfacial tension in practical fluxes.

Acknowledgment

This work was sponsored by the member companies of the Center for Iron and Steelmaking Research at Carnegie Mellon University and the National Science Foundation under tie-project EEC 9417436.

References

1. A. W. Cramb and M. Byrne: "Tundish Slag Entrainment at Bethlehem's Burns Harbor Slab Caster," Transactions of ISS, Vol 10, (1989), p 121 - 128.

2. M. Byrne, A. W. Cramb and T. W. Fenicle: "The Sources of Exogenous Inclusions in Continuous Cast, Aluminum Killed Steels," Transactions of ISS, Vol 10, (1989), p 51 - 60.

3. M. Byrne and A. W. Cramb: "Operating Experiences with Large Tundishes", Transactions of ISS, Vol 10, (1989), p 91 - 100.

4. S. Feldbauer and A. W. Cramb: "Insights into Slag Entrainment in the Mold of a Continuous Caster", 13 th, PTD Conference, Nashville, TN, 1995, p 327 - 342

5. J. M. Harman and A. W. Cramb: "A Study on the Effect of Fluid Physical Properties on Droplet Emulsification", Steelmaking Conference Proceedings, Vol. 79, 1996, p 773 - 784.

6. N. A. McPherson and S. L. McIntosh:"Mold Powder Related Defects in Some Continuously Cast Steel Products," 70th ISS Steelmaking Proceedings, Pittsburgh, PA, 1987, p 17 - 26.

7. A. Kusano, N. Sato, M. Okimori, M. Sato, Y. Minagawa, "Improvement of Mold Fluxes for Stainless and Titanium Bearing Steels," 74th ISS Steelmaking Conference, Washington, D.C., 1991, p 147 - 151.

8. I. Jimbo, B. Ozturk, S. Feldbauer and A. W. Cramb: "Some Aspects of Chemical Phenomena in the Mold of a Continuous Slab Caster", ibid, p 153- 162.

9. R. Bommaraju, T. A. Jackson, J. Lucas, G. Skoczlas, B. Clark, "Design, Development,

and Application of Mold Powder to Reduce Slivers," 75th ISS Steelmaking Conference, Toronto, ON, 1992, p 23 - 31.

10. H. Nakato, S. Takeuchi, T. Fujii, T. Nozaki, M. Washio, "Characteristics of New Mold Fluxes for Strand Casting of Low and Ultra Low Carbon Steel Slabs," 74th ISS Steelmaking Conference, Washington, D.C., 1991, p 639- 646.

11. Y. Tanizawa, M. Toyoda, K. Takatani, T. Hamana, "Behaviour of Second Phase Particles in Continuous Casting Process", La Revue de Metallurgie - CIT, July/August, 1993, p 993-1000.

12. M. M. Wolf, "Advances in Clean Steel Technology", Steel Times, September, 1992, p 408-412.

13. R. C. Sussman, M. T. Burns, X. Huang, B. G. Thomas, "Inclusion Particle Behavior in a Continuous Slab Casting Mold," ISS Process Technology Conference, Vol. 10, Toronto, ON, 1992, p 291 - 304.

14. K. Tanizawa, F. Yamaguchi, K. Inoaka, K. Inaoka, K. Tanaka, "Influence of the Steelmaking Conditions on Nonmetallic Inclusions and Product Defects," First European Conference on Continuous Casting, Florence, Italy, September, 1991, Vol.1, p491-500.

15. H. Matsuda, H. Yasunaka, K. Ayata, N. Genma, M. Kimura, T. Saito, H. Fukumoto, "A New Technique for Decreasing Inclusions in Curved -Type Slab Continuous Casters," 73rd ISS Steelmaking Conference, Detroit, MI, 1990, p 187 - 194.

16. J. Yamasaki, "Production of High Quality Continuously Cast Slab by Mizushima ,No. 4 CCM," CAMP - ISIJ, Vol. 6, 1993, p. 1115.

17. T. Teshima, M. Osame, K. Okimoto, Y. Nimura, "Improvement of Surface Property of Steel at High Casting Speed," 71st ISS Steelmaking Conference, Toronto, ON, 1988, p 111- 118.

18. H. Nakamura, S. Kohira, J. Kubota, T. Kondo, M. Suzuki, Y. Shiratani, "Technology for Production of High Quality Slab at High Speed," 75th ISS Steelmaking Conference, Toronto, ON, 1992, p 409 - 415.

19. T. Teshima, M. Osame, K. Okimoto, Y. Nimura, "Improvement of Surface Property of Steel at High Casting Speed". Steelmaking Conference Proceedings, 1988, Vol 71, p 111-118.

20.H. Tanaka, H. Kuwatori, R. Nisihara, "Analysis of Continuous Casting Powder Entrapping Phenomena by Water - Model Experiments". Iron and Steel Society of Japan, 1992.

21. I. Manabu, S. Yutaka, O. Ryusuke, M. Zen-ichiro, "Evaluation of the Critical Gas Flow Rate Using Water Model for the Entrapment of Slag into a Metal Bath Subject to Gas Injection". Tetsu - To - Hagane, 1993, Vol. 79, No. 5, p 33

22. H. Nakato et al: Continuous Casting- Vol 6, Iron and Steel Society Publication, (1992) p 193-197.

23. J. Herbertson, Q.L. He, P.J. Flint and R.B. Mahapatra: "Modelling of Metal Delivery to Continuous Casting Molds", Mold Operation for Quality and Productivity, Iron and Steel Society, 1991, p 135-149.

24. J. Kubota et al.: "Mechanism of Level Fluctuation and Mold Powder Catching in Slab Casting at high Casting Speeds, Sixth International Iron and Steel Congress Proceedings, Vol. 1, p 356-362.

25. J. Kubota, N. Okoimoto, A. Shirayama and H. Murakami: "Meniscus Flow Control in the Mold by Travelling Magnet Field for High Speed Slab Caster",Mold Operation for Quality and Productivity, Iron and Steel Society, 1991, p 197-205.

26. K. Marukawa and H. Kasima: "The Challenge of Braking the Limit of Steel Refining in Mass Production", The Refining Limit of Impurity Elements in Mass Production, ISIJ, 1996, p 1 - 4.

27. J. Harman, MS Research, Carnegie Mellon University. Pittsburgh, 1996.

28. P. Kozakevich and G. R. Urbain: Mem. Sci. Rev. Metall. , **58,** (1961), pp.517-34.

29. B. F. Dyson: Trans. Met. Soc. AIME, **277**, (1963), pp.1098-1102.

30. F. A. Halden and W. D. Kingery: J. Phys. Chem., **59**, (1955), pp.557-59.

31. Van Tszin-Tan, R. A. Karasev, and A. M. Samarin: Izv. Akad. Nauk SSSR, Met.: Toplive, No. 2, (1960), pp.49-52.

32. H. Gaye, L. D. Lucas, M. Olette, and P. V. Riboud: Can. Met. Quart., **23**, (1984), pp.179-91.

33. K. Ogino, S. Hara, T. Miwa, and S. Kimoto: Trans. Iron Steel Inst. Jpn., **24**, (1984), pp.522-31.

34. I. Jimbo and A. W. Cramb: Proceedings of the Sixth International Iron and Steel Congress, The Iron and Steel Institute of Japan, (1990), pp.499-504.

35. I. Jimbo and A. W. Cramb: ISIJ International, **32**, No. 1, (1992), pp.26-35.

36. A. Kasama, A. McLean, W. A. Miller, Z. Morita, and M. J. Ward: Can. Met. Quart., **22**, (1983), p.9.

37. B. Von Szyszkowski: Z. Phys. Chem., **64** , (1908), pp.385-414.

38. G. R. Belton: Metall. Trans. B, **7B** , (1976), pp.35-42.

39.A. Sharan, T. Nagasaka and A. W. Cramb: Surface Tensions of Fe-Cr and Fe-20%Cr-N alloys: Met Trans B, Vol 25B, 1994, p 626-628

40. A. Sharan and A. W. Cramb: "Interfacial Tensions of Liquid Fe-Ni Alloys and Stainless Steels", Met Trans B, Vol 26 B, 1995, p 87-94

41. A. Sharan: "Surface and Interfacial Tensions of Iron and Nickel Alloys", Phd Thesis, 1994, Carnegie Mellon University

42. C. Dumay and A. W. Cramb: "Densities and Interfacial Tension of Liquid Fe-Si Alloys" Met Trans B, Vol 26 B, 1995, p 173-176

43. T. E. Gammal and U. Schoneberg: Stahl und Eisen, 1992, Vol 1, p 10-18.

44. H. Gaye, L. D. Lucas, M. Olette, and P. V. Riboud: Can. Met. Quart., **23**, (1984), pp.179-91

45. P. V. Riboud and L. D. Lucas: "Influence of Mass Transfer Upon Surface Phenomena in Iron and Steelmaking", Can Met Quart , 20, 1981 p 199-208.

46. I. Jimbo, Y. Chung and A. W. Cramb: "Interfacial Tensions of Liquid Iron-Alloys and Commercial Steels in Contact with Liquid Slags" ISIJ, to be published, 1997.

47. Y. Chung, Masters Research Work at Carnegie Mellon University, 1996.